RSC Advances

PAPER

View Article Online
View Journal | View Issue

Cite this: *RSC Adv.*, 2015, **5**, 91937

Microorganism inspired hydrogels: fermentation capacity, gelation process and pore-forming mechanism under temperature stimulus†

Bingjie Chen,[a] Shuhua Zhang,[b] Qingsong Zhang,*[ac] Qifeng Mu,[b] Lingli Deng,[b] Li Chen,[a] Yen Wei,*[c] Lei Tao,[c] Xiaoyong Zhang[c] and Ke Wang[c]

Received 20th August 2015
Accepted 20th October 2015

DOI: 10.1039/c5ra16811b

www.rsc.org/advances

Learning from the idea of food fermentation, a facile and environmentally benign method has been developed for the preparation of 3D microorganism inspired hydrogels (MIH). To clarify the effect of temperature on the fermentation capacity of yeast, bubble coalescence, gelation time, pore shape and swelling behavior of MIH, a series of temperatures from 25 °C to 50 °C were set to synthesise super-/macro-porous polyacrylamide (PAM) hydrogels with fast response and hierarchical pore structure *via* an environmental friendly fermentation method. It is found that the gelation process of acrylamide and CO_2 gas foaming process of yeast fermentation play decisive roles in controlling the pore structure and swelling behavior of PAM hydrogels. A mutual benefit on the fermentation and unique porous structure make HSYT hydrogels potentially applicable for drug delivery systems, food industries and chemical separation.

1. Introduction

Due to great advantages of a super-/macro-porous structure, fast swelling rate and high elasticity, three-dimensional (3D) porous hydrogels show attractive potential in drug delivery systems, tissue engineering, wastewater treatment and biocatalysis.[1–7] Several excellent reviews on 3D porous hydrogels have been reported by Annabi, Elbert and Omidian.[8–11] The various methods of forming porous hydrogels, such as the pore forming agent method,[12,13] emulsion templating method,[14–16] phase separation,[17,18] and gas forming method have been reported and reviewed by Mikos.[19]

However, the methods above exhibit various problems. For example, Tsioptsias *et al.* adopted the supercritical fluids technique to prepare porous hydrophilic polymers, but high pressures from 50 to 110 bar and complicated equipment were needed.[20] le Droumaguet *et al.* prepared engineering functional doubly porous poly (hydroxyethyl methacrylate)-based materials by using microparticles and nanoparticles straightforwardly, but the porosity were low (from 39% to 61%).[21] Therefore, it is the most urgent task to find an effective method to prepare 3D porous hydrogels. In fact, porous hydrogels can be thought as a viscoelastic matrix, like bread or steamed bun. Learning from this, Zhang *et al.* firstly proposed microorganism inspired hydrogels (MIH) with high adsorption for cationic dye crystal violet, which were prepared by yeast fermentation.[22] In this system, living organism called yeast can metabolize sucrose by breaking some chemical bonds of sucrose and generate gaseous metabolites carbon dioxide (CO_2) constantly, which is served as porogen to prepare porous hydrogels. Instant dry yeast is also called budding yeast or *Saccharomyces cerevisiae*. It's the common yeast used in baking and brewing. The yeast fermentation method combining microorganism and polymer has significant benefits, such as a simplified operation process, rapid pore formation, relatively inexpensive reagents, formation of a larger specific surface area and high adsorption capacity. Chang *et al.* prepared porous channel-like TiO_2 with living yeast cells and their metabolites as promising porogen, and the obtained meso-/macro-porous TiO_2 could be used as anode material for Li-ion battery.[23]

However, there are still many questions to be resolved. It is known to all that fermentation conditions like temperature, pH value, pressure, nutrition, oxygen and reaction time have a significant impact on fermentation of yeast, subsequently leading to uncontrollable pore size or distribution. Especially, the fermentation temperature directly affects the biochemical reactions metabolism and porosity of resulting hydrogels.[24,25] In fact, the fermentation of sucrose is an enzymatic reaction which is significantly affected by temperature. According to published documents or information, it is reported that yeast cells will not grow at 0–10 °C, but grow and multiply at 10–37 °C, with an

[a]State Key Laboratory of Separation Membranes and Membrane Processes, School of Materials Science and Engineering, Tianjin Polytechnic University, Tianjin 300387, China. E-mail: zqs8011@163.com

[b]College of Textile, Tianjin Polytechnic University, Tianjin 300387, China

[c]Department of Chemistry, Tsinghua University, Beijing 100084, China. E-mail: weiyen@tsinghua.edu.cn

† Electronic supplementary information (ESI) available. See DOI: 10.1039/c5ra16811b

optimal growth at 30 or 37 °C (that depends on the species). With increasing temperature above 37 °C, the yeast cells become damaged with some self-repairing capability.

To the best of our knowledge, although the relationship between the yeast and temperature has been clarified, the effect of fermentation temperature upon the fermentation capacity or gelation process of porous hydrogels is still unknown. Therefore, according to above analyses, a series of temperature were set up to prepare polyacrylamide (PAM) hydrogel by simultaneously free radical polymerization in aqueous solution and fermentation of yeast. In this work, production rate of CO_2 and coalescence of bubbles during fermentation triggered by temperature was monitored and investigated by optical microscope and fermentation tube. The gelation of AM under temperature stimulus was observed by rheometer. The effect of temperature on the pore morphology and swelling behavior were investigated by SEM, mercury porosimetry and gravimetric method. The great advantage of porous structure, low cost, easy process and low toxicity allows these 3D porous hydrogels to be an attractive material for applications in food industries, chemical separation and drug delivery.

2. Experimental

2.1 Materials

Monomer acrylamide (AM) and initiator ammonium persulfate (APS) were purchased from Tianjin Fengchuan Chemical Reagent Technology Co., Ltd. Cross-linker *N*,*N*′-methylene-bisacrylamide (MBA) was supplied by Tianjin Kemel Chemical Reagent Co., Ltd. *N*,*N*,*N*′,*N*′-Tetramethylenediamine (TEMED) was obtained from Shanghai Chemical Reagent Co., Ltd. Instant dry yeast and sucrose was purchased from Angel Yeast Co., Ltd. and Shanghai department store (Group) Co. Ltd. respectively. All reagents were analytical grade and used without further purification.

2.2 Preparation of yeast-inspired porous PAM hydrogels under temperature stimulus

The instant dry yeast was used as porogen during polymerization process for foaming. Before polymerization, 1 g yeast was cultivated in 10 mL warm sucrose solution (0.5 g sucrose) with gentle stirring to activate from their dormant state at 30 °C. Then, 2 g AM monomer was first diluted with 10 mL deionized water, followed by the addition of cross-linker MBA (10 wt% with respect to AM). Thereafter, rehydration solution was slowly poured into a glass culture dish containing MBA/AM aqueous solution. Then, a series of temperature, such as 25 °C, 30 °C, 35 °C, 40 °C, 45 °C and 50 °C was set for water bath. Afterward, redox couples of 0.01 g APS and 160 μL TEMED (2% v/v) were added to above mixture solution under gentle stirring to initiate polymerization.

The glass culture dish retaining several gas-guide holes was sealed for polymerization at predetermined temperature, lasting for 4 h. The resulting hydrogels were simply named HSYT, H means hydrogel, S means sucrose, Y means yeast and T means temperature, like HSY25, HSY30, HSY35, HSY40, HSY45, HSY50 represent yeast-inspired hydrogels prepared at 25 °C, 30 °C, 35 °C, 40 °C, 45 °C and 50 °C, respectively. The prepared HSYT hydrogels were subsequently cut into disks approximately with a diameter of 10 mm, and then immersed in deionized water for removing impurities.

2.3 Fermentation of yeast and CO_2 amount under predetermined temperature

To analyze the effect of temperature on the fermentation capacity of yeast, a series of temperature was set to monitor the yield and production rate of CO_2. As yeast ferments the sucrose anaerobically mainly, the CO_2 occupies some volume within the closed system of the fermentation tubes, and the production of CO_2 was recorded by measuring the displacement of prepared solution placed in a fermentation tube. The solution in which the solubility of CO_2 was poor contained 10 wt% NaCl and 1 v/v% H_2SO_4.

Apparent attenuation is used more commonly because it is easier to compute by using volume readings. This volume change was used to monitor the fermentation rate. Volume measurements of released CO_2 during fermentation are taken through displacement of water. To wake yeast from dormant state, yeast must bring a certain amount of water through their cell walls and into the cell. A water bath was simply a large beaker of water at a given temperature to ensure that the baker's yeast was remained at a constant and controlled temperature. 0.5 g sucrose and 1 g yeast were added into 20 mL deionized water in the bottle. After stirring the mixture gently for 5 min at 30 °C, the bottle was set in the water bath under a given temperature. Subsequently the sealed bottle was collected to the draining device. The production amount of CO_2 during specific time intervals was collected for 90 min.

2.4 The bubbles propagation during fermentation of yeast under various temperatures

Yeast was dispersed into 10 mL sucrose solution, and the weight ratio of sucrose/yeast was controlled to 50 wt%. After stirring for 5 min, a drop of yeast fermentation liquid was dropped onto the slides at 25 °C and 50 °C with a coverslip. The whole fermentation process was observed by inverted fluorescence microscope (Ti-U, Nikon Co., Japan).

2.5 Rheological measurements

The rheological measurements during isothermal polymerization were determined by oscillatory shear measurements performed on an ARG2 rheometer (TA instruments, USA) with titanium cone-plate geometry (20 mm diameter). The experiments were carried out with 1% strain and an angular frequency of 1 Hz. The crossover point between storage (G') and loss (G'') moduli was defined as the gel time (t_{gel}). Steady shear tests were carried out at 25 °C, 35 °C and 50 °C on the pure pre-polymerization solutions. The time dependences of G' and G'' of the PAM hydrogel pre-polymerization solutions at 25, 35 and 50 °C were measured and analyzed.

2.6 Environmental scanning electron microscope (ESEM)

Fully swollen HSYT hydrogel prepared at various temperature slices were firstly freeze-dried at −60 °C under vacuum for 10 h, and then the cross-section were sputter-coated with gold. Environmental scanning electron microscope (ESEM, Quanta 200, FEI) were used to observe cross section morphology and internal pore structure.

2.7 Mercury intrusion porosimetry (MIP)

The porosity ratio, pore volume, and pore size distribution of the HSYT hydrogels were determined by mercury intrusion porosimetry (MIP, AutoPore IV 9500, Micromeritics Instrument Co. Ltd., USA). The determination of porosity features was based on the Washburn equation between the applied pressure (from 0.51 to 30 kPa) and the pore diameter into which mercury intruded.

2.8 Swelling dynamic behavior

The freeze-dried HSYT hydrogel samples were put into deionized water at 25 °C, and weighed after wiping the excess surface liquid by filter paper at predetermined intervals. The swelling ratios (SR) at predetermined time were calculated by eqn (1),

$$\mathrm{SR} = \frac{m_t - m_\mathrm{d}}{m_\mathrm{d}} \times 100\% \quad (1)$$

where m_d is the weight of freeze-dried sample, and m_t is the weight of the swollen sample at time t.

2.9 Confocal scanning microscope (CSM)

Fully swollen HSYT hydrogel slices were firstly freeze-dried at −60 °C under vacuum for 10 h, and then the cross-section of HSYT hydrogels were stick to the glass slide. Confocal scanning microscope (CSM, ZEISS Axio CSM 700, Germany) was used to observe the distribution of the yeast on the cross section.

3. Results and discussion

3.1 The bubbles' shape under fermentation process at 25 °C and 50 °C

It's much better that sucrose is severed as carbon resource of active dry yeast cells because just little amount of sucrose is enough unlike glucose. In fact, sucrose can be converted to glucose and fructose by the invertase.[26,27] The invertase, distributed on the cell wall or within the cell, works together to ensure efficient fermentation of sucrose.[28] And finally gaseous metabolized CO_2 and alcohol were produced during fermentation *via* aerobic and anaerobic respiration.

$$C_6H_{12}O_6 + 6H_2O + 6O_2 \rightarrow 6CO_2 + 12H_2O + \text{energy}$$

$$C_6H_{12}O_6 \rightarrow 2C_2H_5OH + 2CO_2 + \text{energy}$$

Due to significantly affect upon the creation of the porous structure, further insight about the bubbles is required. The optical microscope is sufficient to solely look at the bubble generation of yeast in sucrose solution.[29] To observe the change of bubbles generated by CO_2, optical microscopic images of yeast/sugar mixture solution were taken. Fig. 1 shows the bubbles' appearance during fermentation process at 25 °C and 50 °C. It is seen that CO_2 bubbles were generated at 50 °C after fermenting 1 min, while no bubbles were observed at 25 °C within 4 min. Once a bubble occurs, it's too fast to capture the growing process. The bubble size fermenting at 25 °C for 14 min is close to that at 50 °C for 3 min. It indicates that the increase of temperature can accelerate foaming speed of CO_2 gas. This probably because that

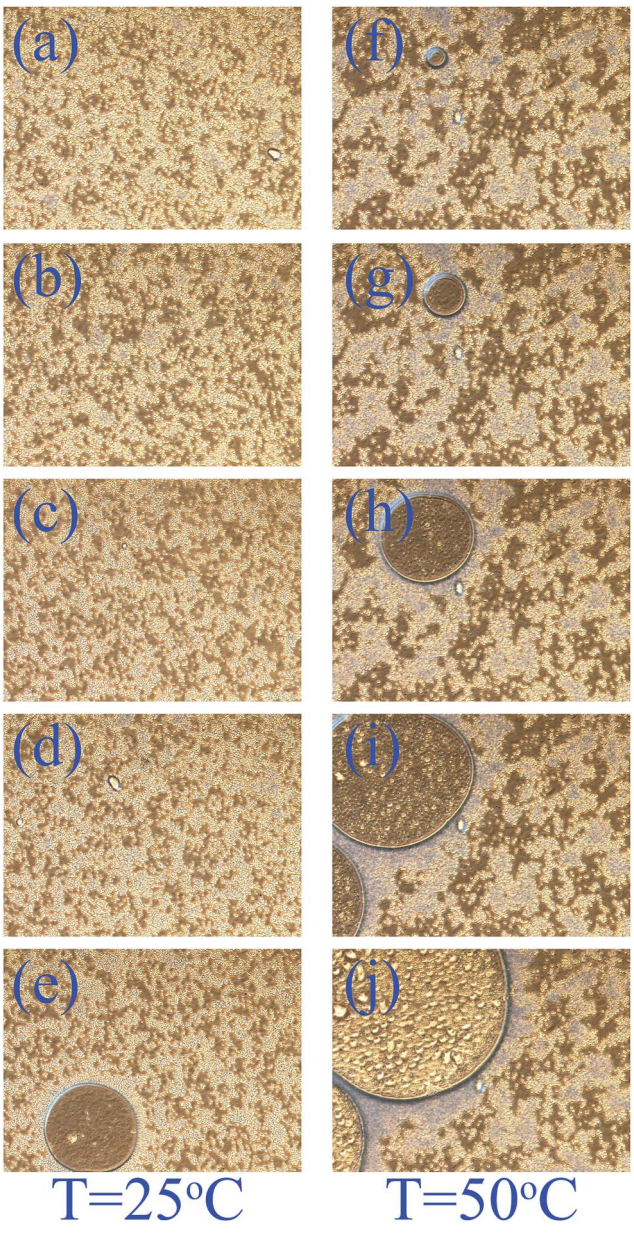

Fig. 1 The bubbles' appearance during fermentation process at 25 °C and 50 °C observed by the microscope in the video mode. The weight ratio of sucrose/yeast was controlled to 50 wt%. (a) 1 min; (b) 2 min; (c) 3 min; (d) 4 min; (e) 14 min; (f) 1 min; (g) 2 min; (h) 3 min; (i) 4 min; (j) 5 min.

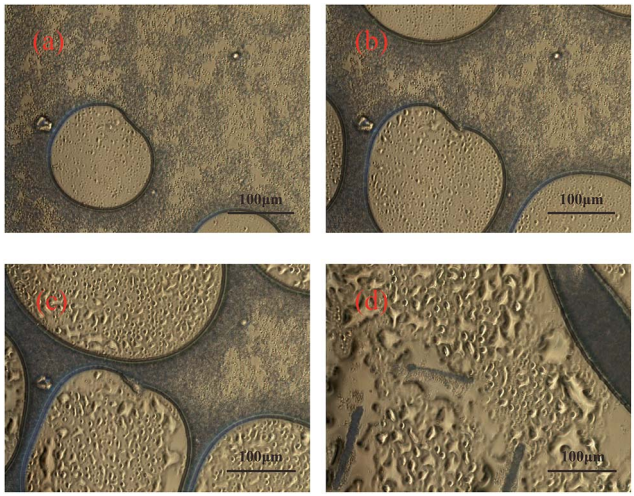

Fig. 2 The mergence among bubbles during the fermentation process observed by microscope in the video mode at 40 °C. (a) Single bubble; (b and c) growing bubbles; (d) merged bubbles. The weight ratio of sucrose/yeast was controlled to 50 wt%.

the activation time of yeast at 50 °C is shorter than that at 25 °C. The faster the gaseous CO_2 produced, the shorter time and larger amount the visible bubbles could be observed.

Furthermore, it is of interest to note that, with further increasing fermentation time, the mergence among bubbles during the growth of bubbles can be found. As shown in Fig. 2, by merging nearby small bubbles, larger bubbles were obtained. The generated bubbles push the yeast cells clump together around the interface of bubbles and fermentation mixture. It is certainly to assume that the sizes of bubbles are not uniform on account of differences in fermentation temperature, merged bubbles number and dead yeast cell counts. Therefore, it is reasonable to conclude that the sizes of bubbles after fermentation are hierarchical due to the coalescence of adjacent bubbles.

3.2 Generated CO_2 amount and rate at different fermentation temperature

As mentioned above, the CO_2 amount produced by yeast and sucrose was dependent on fermentation temperature, efficient fermentation of sucrose by yeast cells is crucial for hydrogels leavening. And by measuring the produced rate and volume of the CO_2, the fermentation efficiency *via* enzymatic action under

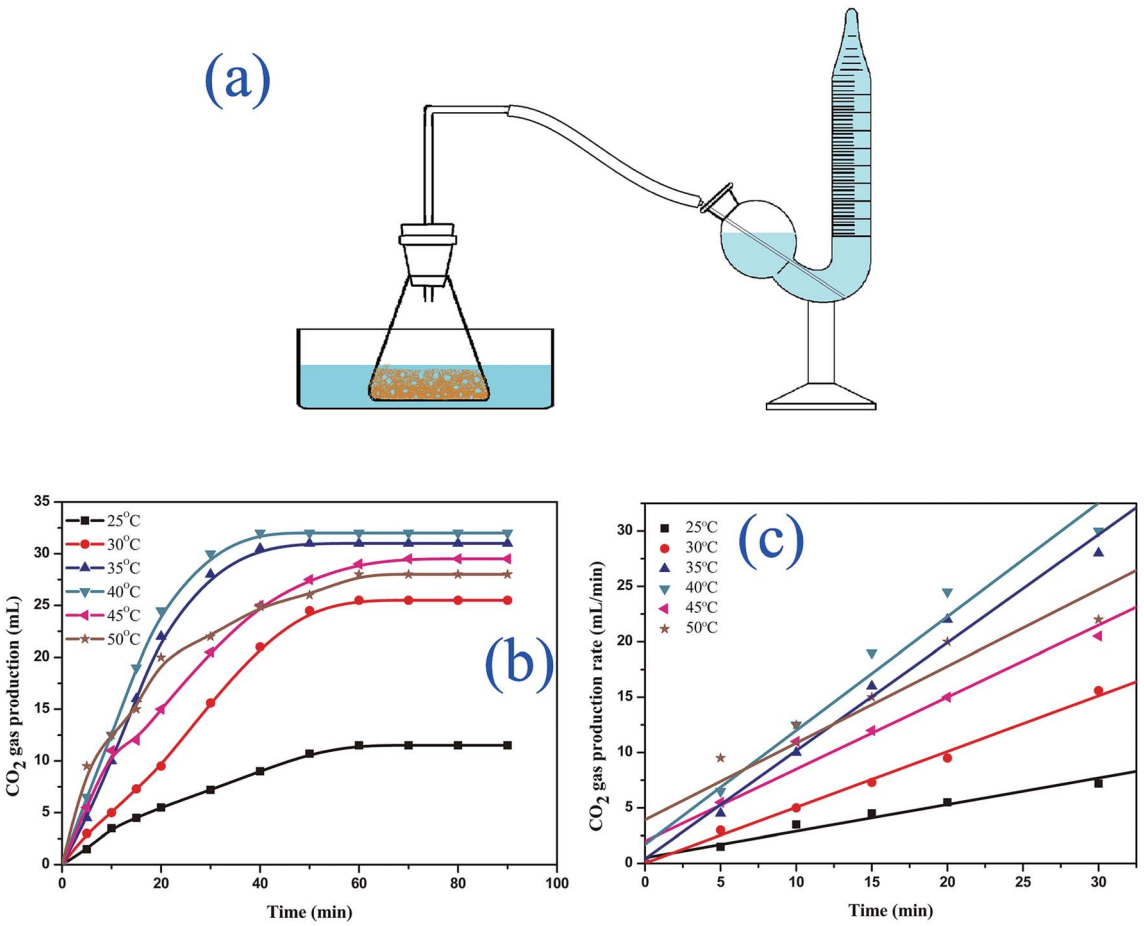

Fig. 3 The measuring equipment of gas yield of CO_2 (a). CO_2 gas amount produced by yeast fermentation at different temperatures as a function of fermentation time (b); the linear fitting curve ofthe gas production within 30 min (c). The fermentation solution contained 0.5 g sucrose, 1 g yeast and 20 mL deionized water.

different temperature can be obtained. Fig. 3 shows the CO_2 amount produced by yeast fermentation at temperature ranging from 25 to 50 °C as a function of fermentation time. As shown in Fig. 3(a), with increasing fermentation time from 0 to 90 min, the generated CO_2 gas increases quickly before 60 min and then keeps almost constant. At 25 °C, the CO_2 amount is just 11.5 mL after fermentation for 60 min. But at 30 °C, the CO_2 amount generated by yeast fermentation increases greatly, which is 2.2 times of that at 25 °C. With increasing fermentation temperature from 35 °C to 40 °C, the CO_2 amounts increase to 32 and 31 mL after fermentation for 40 min. However, when fermentation temperature is at 45 °C and 50 °C, the CO_2 amounts began to decrease. The reason can be ascribed to the enzyme catalysis process during fermentation. Enzyme is extremely sensitive to temperature. In fact, some of the enzyme in the yeast cell would denature over 60 °C. As reported by Won *et al.* that the optimum temperature of fermentation process for the most common yeast, *Saccharomyces cerevisiae*, is between 30 °C and 37 °C.[30] The amounts of gas generated by yeast in dough measured at 25 °C to 40 °C show the same increasing effect of temperature on the fermentative activity.[31] Mamun-Or-rashid *et al.* also pointed that the loss of fermentative activity of dry yeast increased with increasing temperature from 45 °C to 85 °C.[32] Therefore, it is reasonable to assume that the optimum temperature for producing sufficient CO_2 is 35 °C to 40 °C.

To further study CO_2 production rate at various fermentation temperatures, the CO_2 amount within 30 min was linear fitted, as shown in Fig. 3(b). The value of the slope of these straight lines reflects the average rate of bubble growth at different temperature. The slopes are 0.24, 0.50, 0.96, 1.03, 0.65 and 0.69, respectively. It indicates that, at 35 °C and 40 °C, the fermentation speeds are the fastest and the CO_2 production amount are the largest.

3.3 The influence of temperature on PAM hydrogel gelation time

Fig. 4 shows time evolution of G' and G'' at 25, 35 and 50 °C for pure PAM hydrogels. It is seen that, with increasing polymerization time from 0 to 30 min, both G' values of PAM pre-polymerization solution measured at 25, 35 and 50 °C increase significantly at a certain time, while G'' values keep almost the same. The increasing G' values indicate the formation of solid hydrogel network. According to the definition of gelation time (t_{gel}), the t_{gel} values can be determined. And t_{gel} values of PAM hydrogels prepared at 25, 35 and 50 °C are about 25, 15 and 7.5 min. It suggests that higher reaction temperature can accelerate the polymerization of AM/MBA system and short the reaction time. Ahmed has also pointed out that the gelation time decreased with an increase in temperature and the temperature dependence of gelation could be represented by an Arrhenius equation.[33] Due to the same usage of APS-TEMED redox initiation system, the activation energy of AM/MBA reaction system decreases with increasing from 25 °C to 50 °C. As a result, the polymerization triggered at higher temperature by a faster polymerization rate from 25 °C to 50 °C. However, it should be noted that higher temperature does not mean the increase of the elastic deformation ability. As shown in Fig. S1,† G' values of HSYT hydrogels increased firstly, and then decreased with the increase of temperature form 25 °C to 50 °C. MIH does not significantly enhance the storage modulus compare to pure gelation method although it shows partial increase of the elastic deformation ability according to rheological data (Fig. S1†).

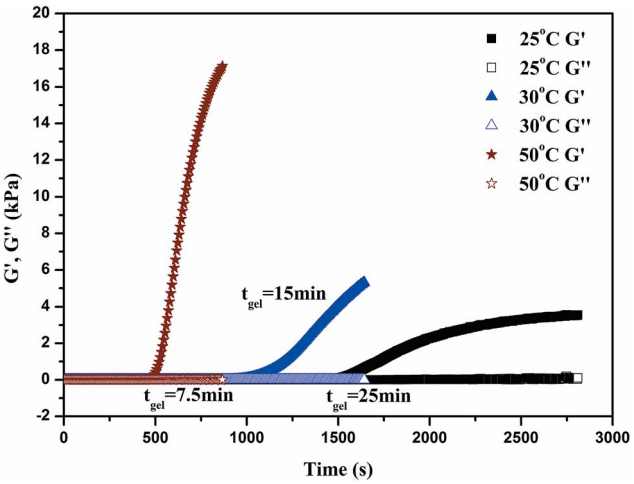

Fig. 4 The time evolution of G' and G'' for PAM pre-polymerization solutions prepared at 25, 35 and 50 °C. The measurement was conducted at strain of 1% and an angular frequency of 1 Hz.

3.4 The appearance of HSYT hydrogels at freeze-dried and swollen state

In this experiment, by using CO_2 as foam produced by fermentation between yeast and sucrose, the porous hydrogels with various pore size and pore shape were prepared under gelation of AM/MBA reaction system and fermentation of yeast. Fig. 5 shows the appearance of HSY25, HSY35 and HSY50 in dried and fully swollen state. It is seen that all HSYT samples show pale yellow due to the existence of yeast cells. However, it is found that the pore structure has close relationship with reacted temperature. In view of pore shape for HSYT hydrogels in dried state, different pore structure and shape are clearly to be found. HSY25 presents both bigger pore (900 μm) and smaller pore, while HSY35 shows well-distributed pore structure (approximately 500 μm). The obvious difference in pore size and pore shape maybe because of temperature, higher temperature will accelerate the polymerization of acrylamide and fermentation of yeast. As described in Fig. 4, the formation time of the network decreased significantly with increasing temperature from 35 °C to 50 °C. As seen in Fig. 3, at 35 °C and 40 °C, the fermentation speeds are the fastest and the CO_2 production is the largest. The competitive result of gelation of acrylamide and fermentation of yeast leads to various pore structures of HSYT hydrogels.

3.5 The pore shape and porosity of HSYT hydrogels stimulated by temperature

The temperature affects the gelation time and ability of the reaction system to hold gas, which plays a key role in controlling

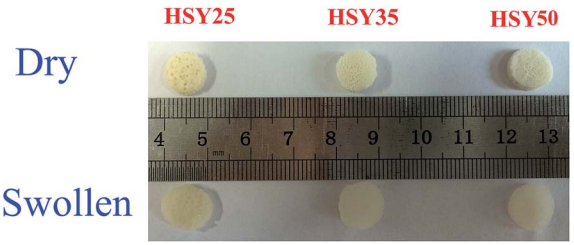

Fig. 5 Appearance of HSYT hydrogel in dried and fully swollen state prepared at various temperature. There are HSY25, HSY35 and HSY50, respectively, from left to right.

the pore size and shape of HSYT hydrogels. Fig. 6 shows ESEM images of HSYT hydrogels at various fermentation temperatures. It can be found that HSYT hydrogels exhibit hierarchical pore structure with diameter ranging from 5 to 900 μm. For HSY25 hydrogel, there are both bigger (600–900 μm) and smaller pores (20–100 μm). Especially, the pore wall between bigger pores also exist numerous small pores. At 25 °C, the CO_2 generation rate and gelation process are all slowest. 4 h later, large amount of fibrous thread can be found from ESEM graphs. It indicates that gelation of HSY25 hydrogel at 25 °C is uncompleted, leading to lower capacity of holding gas of HSY25 hydrogel network. In this case, macroscopic state and interior shape are all uneven. At 30 °C, the CO_2 gas production amount increases obviously, while gelation rate still keeps at a lower value. As a result, HSY30 hydrogel exhibits biggest pores with diameters from 500 to 700 μm. Here, any fibrous thread can't be found, which indicating that the reaction temperature at 30 °C increases the polymerization capability of AM/MBA. With further increasing temperature to 35 °C and 40 °C, HSY35 hydrogel present uniform pore structure with a diameter of 400–500 μm. As mentioned in Fig. 3, the optimum temperature for producing enough CO_2 is 35 °C to 40 °C. It is also true that CO_2 gas-holding capacity of the HSY35 hydrogel at this temperature is better due to high reaction activity. In other words, two processes, the gelation process and gas foaming process of yeast fermentation is synchronous in such a way. In that case, the balance between gelation and fermentation enables harmonized foaming and gelation, leading to well-distributed pore structure. As the temperature was controlled at 45 °C and 50 °C, HSY45 and HSY50 hydrogels show hierarchical pore structure with pore diameter from 30 to 100 μm. It is also noteworthy that the pores are interconnecting despite the pore sizes are not uniform. As temperature exceeds 45 °C, the gelation process is very fast, but foaming rate becomes slower. Furthermore, although high temperature can accelerate the foaming of HSYT hydrogels, excessive temperature would lead to early death of yeast cells. Then, in the reaction solutions, small bubbles produced by fermentation were retained in the hydrogel system, resulting in hierarchical pore structure.

Mercury intrusion porosimetry (MIP) can provide a wide range of information, *e.g.* the porosity and specific surface area of a sample. Here, the porosity features of HSY25, HSY35 and HSY50 hydrogels were displayed in Table 1. It is seen that, compared to HSY25 and HSY50 hydrogels, HSY35 hydrogels present the highest porosity at 81.91% and total pore volume at 1.21 $m^2\ g^{-1}$, but only 25.48 μm upon average pore diameter, which is in good agreement with Fig. 6. SEM graphs have confirmed that HSY35 hydrogel possesses the highest holding capacity of CO_2 gas, and presents well-distributed pore

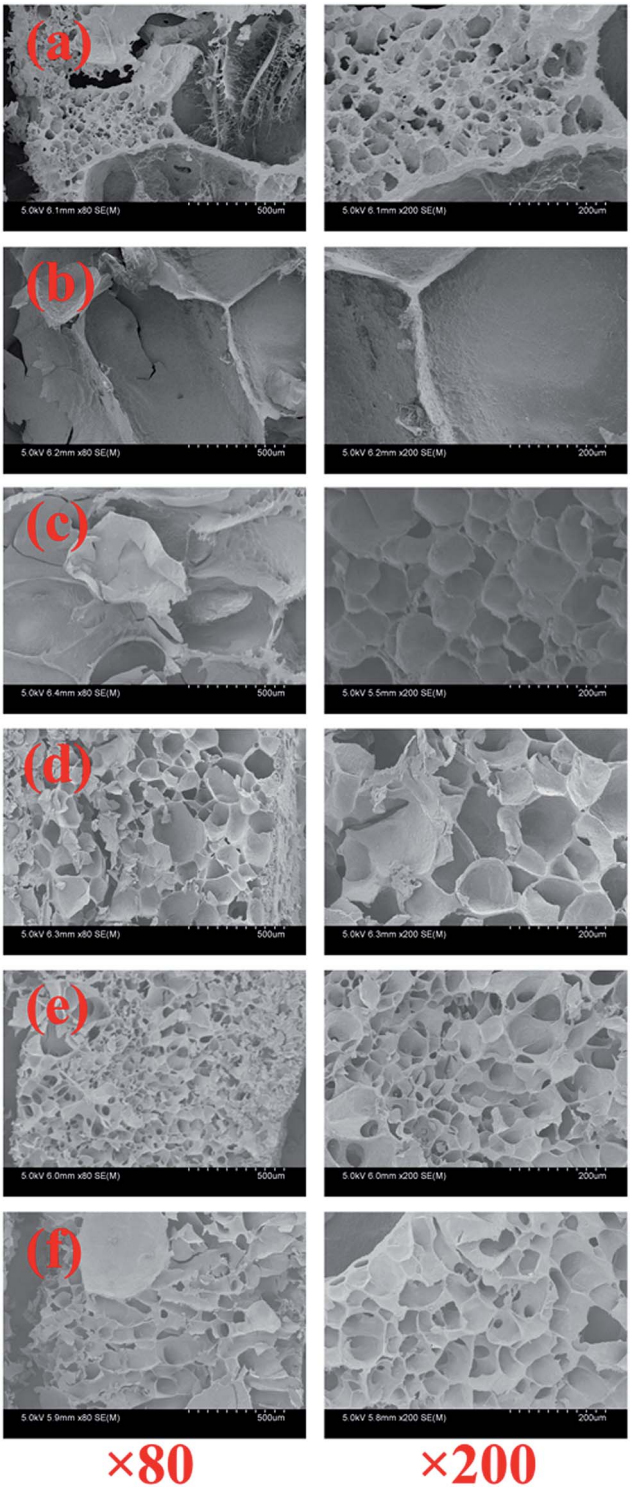

Fig. 6 The ESEM images of HSYT hydrogels at various fermentation temperatures at magnification of 80 times and 200 times. (a) 25 °C; (b) 30 °C; (c) 35 °C; (d) 40 °C; (e) 45 °C; (f) 50 °C.

Table 1 Porosity features of HSY25, HSY35 and HSY50 hydrogels

Code	Porosity (%)	Total pore volumes ($m^2\ g^{-1}$)	Average pore diameters (μm)
HSY25	55.53	0.317	28.21
HSY35	81.91	1.207	25.48
HSY50	78.11	0.201	75.40

structure with a diameter of 400–500 μm. As a result, in a measurement scope of MIP investigation, HSY35 hydrogel shows the smallest average pore diameter. It's true that HSYT hydrogels with bigger pore size and high porosity are beneficial for drug control release, and the related works would be reported in future study.

3.6 Swelling dynamic behaviors of HSYT hydrogels

Swelling is a result of balance between osmotic force and dispersing force. To study the swelling rate upon time, the kinetic curves of swelling ratios (SR) of HSYT hydrogels at 25 °C and fitted curves between $\log(W_t/W_\infty)$ and lg t were obtained as shown in Fig. 7(a) and (b). It is seen that with increasing swelling time from 0 to 280 min, the swelling ratios (SR) values of HSYT hydrogels increase quickly within 50 min and then keep constant. It's noteworthy that HSY25, HSY30 and HSY35 hydrogels have reached equilibrium swelling ratios (ESR) at 50 min, while HSY40, HSY45 and HSY50 hydrogels reach ESR at about 180 min. HSY35 presents the fastest swelling rate, and HSY35 hydrogel has almost reached the maximum ESR values at 20 min, 10.2 g g^{-1}, which is 2.5 and 1.6 times of HSY25 and HSY30 hydrogels, respectively. However, as reaction temperature exceeds 40 °C, the swelling rates and maximum ESR values of HSY40, HSY45 and HSY50 hydrogels decrease. The appearance, SEM images and the MIP data have proven that HSY35 hydrogel presents uniform porous structure and largest porosity, leading to largest ESR value and fastest swelling rate. Due to lower pore size and uneven pore structure, HSY25 hydrogel shows the lowest values of swelling ratios. For HSY40, HSY45 and HSY50 hydrogels, although hierarchical pore structure was found, such heterogeneity leads to rapid swelling rate and lower maximum ESR values.

To further determine the type of water diffusion into HSYT hydrogels, the following eqn (2) were adopted,

$$\lg(W_t/W_\infty \leq 0.6) = \lg(Kt^n) = \lg K + n \lg t \quad (2)$$

where W_t and W_∞ represent the weight of HSYT hydrogel at t and infinite time, respectively. K is a constant related to the network structure and n is the diffusion exponent, which is indicative of the type of diffusion. Fig. 7(b) shows the fitted curves by eqn (2). The n values, calculated slopes of fitted curves, of HSY25, HSY30, HSY35, HSY40, HSY45 and HSY50 hydrogels are 0.26, 0.20, 0.39, 0.20, 0.27 and 0.22, respectively. It is clearly seen that all values of diffusion exponent (n) are below 0.5. Thus the diffusion of water into HSYT hydrogels follows the Fickian diffusion law, and it is the diffusion-controlled process.

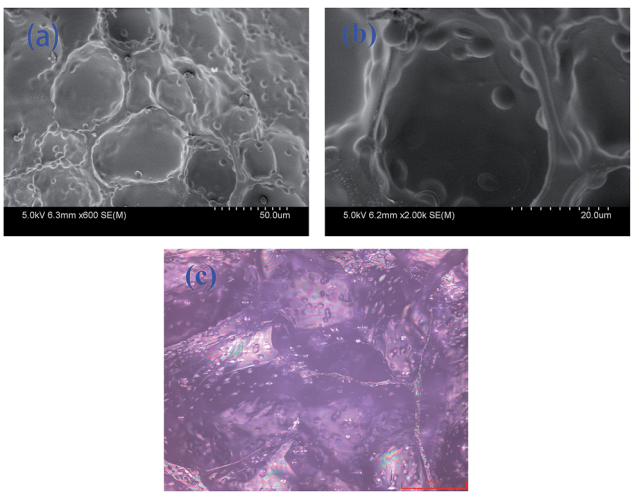

Fig. 8 The yeast cells inside of HSY35 matrix (a): ESEM image of HSY35 at magnification of 600 times; (b): ESEM image of HSY35 at magnification of 2000 times; (c): CLSM image of HSY35 at magnification of 200 times.

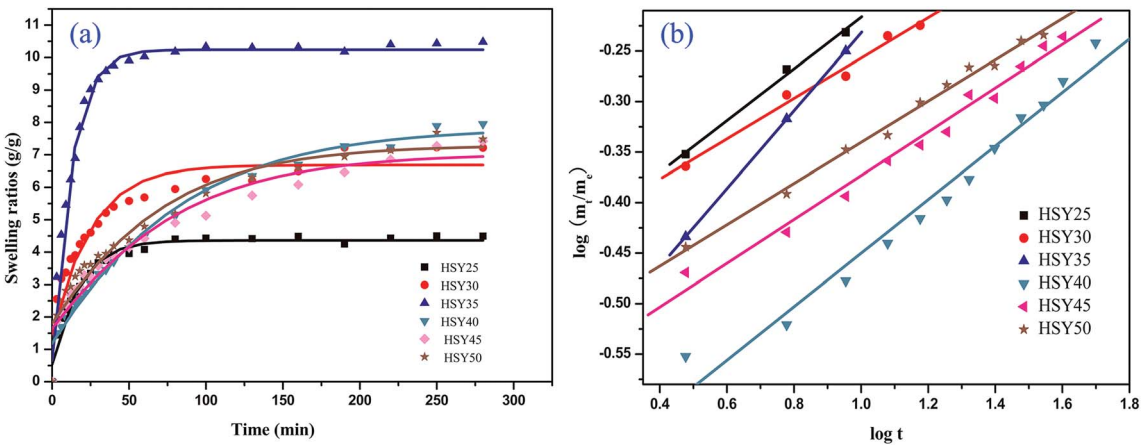

Fig. 7 Swelling dynamics curves of HSYT hydrogels as a function of time at 25 °C (a), the linear fitting curve of the swelling ratio within 30 min (b).

As shown in Fig. 8, large amounts of dead yeast cells gathered in the holes of HSY35 hydrogels. The yeast cells distribute on the pore walls densely, which was in accordance with the distribution of yeast cells in Fig. 2. In the Fig. 2, bubbles coalescence in the fermentation solution was observed and yeasts were pushed together by the bubbles and distribute on the boundary of the bubbles. It indicated that the yeast fermented in the pre-polymerization solution in the same manner as that in the fermentation solution which only contained yeast cells and sucrose. And the unique pore structure was generated by yeasts.

3.7 Polymerization mechanism of HSYT hydrogel under temperature-stimulus

For HSYT hydrogels triggered by temperature, the gelation process of AM/MBA solutions and CO_2 gas foaming process of yeast fermentation play a decisive role in controlling the structure, pore shape and swelling behavior. There must be a best balance between fermentation of yeast and gelation time for the reaction triggered by temperature. The time dependence of gelation process and the CO_2 gas generating process under different temperature was shown in Fig. 9. With increasing temperature from 25 to 50 °C, the gelation time decreases from 25 to 7.5 min, and the production of CO_2 gas increases with time in 40 min. At the gelation point of 25, 35 and 50 °C, the gas production are 6.4, 16 and 11 mL, respectively. At 35 °C, the gas production of CO_2 is the largest, the max swelling ration of HSY35 is the largest in Fig. 7. It is plausible that at 35 °C the utilization of CO_2 gas and gelation time keep the best balance. To further clarify the reaction process and polymerization mechanism, a schematic diagram was given, as shown in Fig. 10. On the one hand, in the fermentation system of yeast/sucrose, a proper temperature is much better for the proliferation of yeast cells and production of bubbles. In fact, excessive high temperature would decrease the activation of enzyme, which is of extremely negative to the fermentation production. According to the results analyzed in Fig. 3, at 35 °C and 40 °C, the fermentation speeds are the fastest and the CO_2 production are the largest. On the other hand, in the reaction system of AM/MBA, once triggered by temperature, a radical polymerization reaction is initiated and the initial poly(AM/MBA) molecular chains are formed. With increasing reaction time, viscosity of the reaction system increases, and cross-linking network is finally obtained. At lower temperature, *e.g.* 25 °C, the gelation

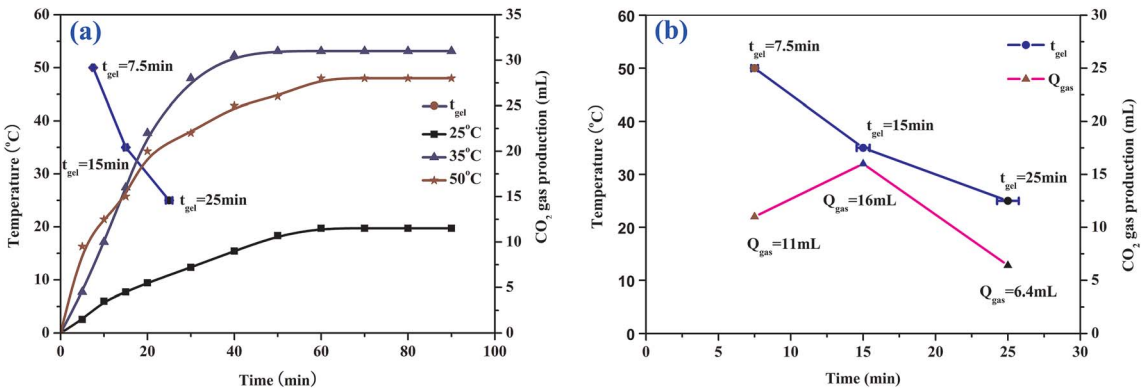

Fig. 9 The harmonization of time-dependent gelation process and the CO_2 gas generating process. The data of figure were from Fig. 3 and 4. With increasing reaction temperature from 25 °C to 50 °C, t_{gel} values of PAM hydrogels decreased from 25 to 7.5 min. Temperature signals at 25 °C, 35 °C and 50 °C were marked with wine, blue and black, respectively (results represented are mean ± SD, $n = 3$). The current error bars are for gelation time.

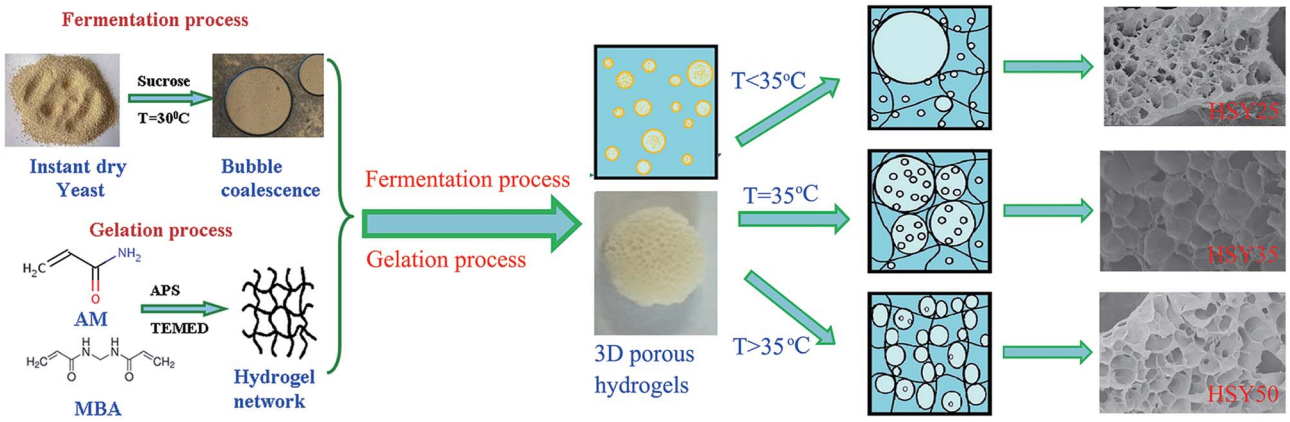

Fig. 10 Polymerization mechanism of HSYT hydrogel under temperature-stimulus.

time of AM/MBA system is longer, capability of 6.4 mL CO_2 gas is available. Accordingly, HSY25 hydrogel present uneven pore structure followed by both bigger pores and smaller pores, and the lowest swelling ratios. At general temperature, like 35 °C, the gelation process and gas foaming process of yeast fermentation is almost synchronous. In this case, HSY35 hydrogel exhibits well-distributed pore structure and the maximum swelling ratios. At high temperature, like 50 °C, the gelation time is 7.5 min. The combination result is that HSY50 hydrogel shows hierarchical pore structure with pore diameter just from 30 to 100 μm and decreasing swelling ratios.

4. Conclusions

This paper confirms the effect of temperature on controlling foaming speed of CO_2 gas and gelation process of hydrogels. The CO_2 bubbles were generated at 50 °C after fermenting 1 min, while no bubbles were observed at 25 °C within 4 min. At 35 °C and 40 °C, the fermentation speeds were the fastest and the CO_2 production amount were the largest. With increasing reaction temperature from 25 °C to 50 °C, t_{gel} values of PAM hydrogels decreased from 25 to 7.5 min. Bubbles of CO_2 gas generate super-/macro-porous structure in all HSYT samples. Due to lower reaction temperature, HSY25 hydrogel presented both bigger (600–900 μm) and smaller pores (20–100 μm), while HSY35 hydrogel presented uniform pore structure with a diameter of 400–500 μm. HSY35 hydrogel reached the maximum ESR values at 20 min, 10.2 g g^{-1}, which was 2.5 and 1.6 times of HSY25 and HSY30 hydrogels, respectively. With increasing reaction temperature from 25 °C to 50 °C, t_{gel} values of PAM hydrogels decreased from 25 to 7.5 min. The combination of low cost, facial preparation and unique hierarchically porous structure holds the promise for drug delivery system, food industries and chemical separation. Considering these results, additional task will be to control the physiological environment for yeast growth and using different biodegradable polymers, other porous materials with unique properties could be obtained.

Acknowledgements

This work is supported by National Nature Science Foundation of China (21104058, 31200719, 21134004 & 21174103), and the grant from the Applied Basic Research, Advanced Technology Programs of Science and Technology Commission Foundation of Tianjin (12JCQNJC01400 & 15JCYBJC18300), Science and Technology Correspondent of Tianjin (14JCTPJC00502) and Tianjin Polytechnic University Innovation Foundation For Postgraduate (15108).

References

1 R. Chen, Q. Chen, D. Huo, Y. Ding, Y. Hu and X. Jiang, *Colloids Surf., B*, 2012, **97**, 132–137.
2 H. Park, K. Park and D. Kim, *J. Biomed. Mater. Res., Part A*, 2006, **76**, 144–150.
3 D. J. Mastropietro, H. Omidian and K. Park, *Expert Opin. Invest. Drugs*, 2012, **9**, 71–89.
4 Q. S. Zhang, P. P. Dong, L. Chen, X. Z. Wang and S. Lu, *J. Biomed. Mater. Res., Part A*, 2014, **102**, 76–83.
5 S. Potorac, M. Popa, V. Maier, G. Lisa and L. Verestiuc, *Mater. Sci. Eng., C*, 2012, **32**, 236–243.
6 Y. Zhang and L. Ye, *Polym.-Plast. Technol. Eng.*, 2011, **50**, 776–782.
7 K. Ueno, K. Matsubara, M. Watanabe and Y. Takeoka, *Adv. Mater.*, 2007, **19**, 2807–2812.
8 N. Annabi, J. W. Nichol, X. Zhong, C. Ji, S. Koshy, A. Khademhosseini and F. Dehghani, *Tissue Eng., Part C*, 2010, **16**, 371–383.
9 D. L. Elbert, *Acta Biomater.*, 2011, **7**, 31–56.
10 H. Omidian, J. G. Rocca and K. Park, *J. Controlled Release*, 2005, **102**, 3–12.
11 H. Omidian, K. Park and J. G. Rocca, *J. Pharm. Pharmacol.*, 2007, **59**, 317–327.
12 B. Strachotova, A. Strachota, M. Uchman, M. Šlouf, J. Brus, J. Pleštil and L. Matějka, *Polymer*, 2007, **48**, 1471–1482.
13 X. Z. Zhang and R. X. Zhuo, *Eur. Polym. J.*, 2000, **36**, 2301–2303.
14 K. Chen, Q. S. Zhang, B. J. Chen and L. Chen, *Appl. Clay Sci.*, 2012, **58**, 114–119.
15 W. J. Gao, Q. S. Zhang, P. F. Liu, S. H. Zhang, J. Zhang and L. Chen, *RSC Adv.*, 2014, **4**, 34460–34469.
16 Z. Bing, J. Y. Lee, S. W. Choi and J. H. Kim, *Eur. Polym. J.*, 2007, **43**, 4814–4820.
17 V. R. Patel and M. M. Amiji, *Pharm. Res.*, 1996, **13**, 588–593.
18 J. L. Holloway, A. M. Lowman and G. R. Palmese, *Soft Matter*, 2013, **9**, 826–833.
19 A. G. Mikos and J. S. Temenoff, *J. Biotechnol.*, 2000, **3**, 23–24.
20 C. Tsioptsias, M. Paraskevopoulos, D. Christofilos, P. Andrieux and C. Panayiotou, *Polymer*, 2011, **52**, 2819–2826.
21 B. le Droumaguet, R. Lacombe, H. B. Ly, M. Guerrouache, B. Carbonnier and D. Grande, *Polymer*, 2014, **55**, 373–379.
22 Q. S. Zhang, B. J. Chen, L. Tao, M. Y. Yan, L. Chen and Y. Wei, *RSC Adv.*, 2014, **4**, 32475–32481.
23 Y. C. Chang, C. Y. Lee and H. T. Chiu, *ACS Appl. Mater. Interfaces*, 2013, **6**, 31–35.
24 M. J. Torija, N. Rozes, M. Poblet, J. M. Guillamón and A. Mas, *Int. J. Food Microbiol.*, 2003, **80**, 47–53.
25 J. P. Zanon, M. F. Peres and E. A. Gattás, *Enzyme Microb. Technol.*, 2007, **40**, 466–470.
26 P. Gélinas, *Recent Pat. Food, Nutr. Agric.*, 2010, **2**, 1–11.
27 U. E. Donalies, H. T. Nguyen, U. Stahl and E. Nevoigt, *Food Biotechnol.*, 2008, 67–98.
28 A. S. Batista, L. C. Miletti and B. U. Stambuk, *Microb. Biotechnol.*, 2005, **8**, 26–33.
29 M. Scanlon and M. Zghal, *Food Res. Int.*, 2001, **34**, 841–864.
30 K. Y. Won, Y. S. Kim and K. K. Oh, *Korean J. Chem. Eng.*, 2012, **29**, 1341–1346.
31 Y. Kyogoku and K. Ouchi, *Appl. Environ. Microbiol.*, 1995, **61**, 639–642.
32 A. Mamun-Or-rashid, B. K. Dash, M. Chowdhury, M. F. Waheed and M. K. Pramanik, *Pak. J. Biol. Sci.*, 2013, **16**, 617–623.
33 A. Fatimi, J.-F. Tassin, R. Turczyn, M. A. Axelos and P. Weiss, *Acta Biomater.*, 2009, **5**, 3423–3432.